RSC Advances

PAPER

View Article Online
View Journal | View Issue

Cite this: *RSC Adv.*, 2018, **8**, 662

Enhanced photocatalytic activity of a B_{12}-based catalyst co-photosensitized by TiO_2 and Ru(II) towards dechlorination†

Ying Sun,[a] Wei Zhang,*[a] Tian-Yi Ma,[b] Yu Zhang,[a] Hisashi Shimakoshi,[c] Yoshio Hisaeda[c] and Xi-Ming Song*[a]

Received 4th December 2017
Accepted 18th December 2017

DOI: 10.1039/c7ra13037f

rsc.li/rsc-advances

A novel hybrid photocatalyst denoted as B_{12}–TiO_2–Ru(II) was prepared by co-immobilizing a B_{12} derivative and trisbipyridine ruthenium ($Ru(bpy)_3^{2+}$) on the surface of a mesoporous anatase TiO_2 microspheres and was characterized by DRS, XRD, SEM and BET *et al.* By using the hybrid photocatalyst, DDT was completely didechlorinated and a small part of tridechlorinated product was also detected in the presence of TEOA only after 30 min of visible light irradiation. Under simulated sunlight, the hybrid exhibited a significantly enhanced photocatalytic activity for dechlorination compared with B_{12}–TiO_2 under the same condition or itself under visible light irradiation due to the additivity in the contribution of UV and visible part of the sunlight to the electron transfer. In addition, this hybrid catalyst can be easily reused without loss of catalytic efficiency. This is the first report on a B_{12}-based photocatalyst co-sensitized by two photosensitizers with wide spectral response.

Introduction

Photocatalysis has played a special role in both pollutant degradation and organic synthesis from the viewpoint of eco-friendliness in recent decades.[1–5] As photocatalysts, vitamin B_{12} and its derivatives have exhibited excellent photocatalytic activity for decomposing halogenated organic compounds due to the supernucleophilic reactivity of Co(I) species, which could be produced from the Co(III) or Co(II) center of B_{12} and its derivatives under ultraviolet light irradiation in the presence of electron donor precursors.[6–11] In 2004, Hisaeda *et al.*[12] firstly reported the photocatalytic activity of a heptamethyl cobyrinate perchlorate, [Co(II)7C_1ester]ClO_4, in methanol for DDT dechlorination under visible light irradiation in the presence of $Ru(bpy)_3^{2+}$ as photosensitizer and proved that the Co(I) species could be formed through accepting electrons from the photosensitizer under visible light irradiation. In order to establish a more efficient, economical and environmental friendly visible-light photocatalytic system, heterogenous catalysis has been performed through immobilizing the B_{12} catalyst and a photosensitizer onto catalyst supports and some recycled hybrid catalysts based on B_{12} were obtained.[13,14] In 2011, Hisaeda group[14] immobilized a B_{12} derivative and trisbipyridyl ruthenium proportionally on the same polymer backbone through radical polymerization reaction, and the obtained copolymer catalyst showed high catalytic activity for dehalogenation reaction. They proved that the electron transfer rate from the photosensitizer to the Co center of the B_{12} catalyst was significantly accelerated attributing to the short distance between the catalyst and the photosensitizer in the copolymer.

TiO_2 as a semiconductor has been widely applied in various fields such as dye-sensitized solar cell, organic pollution degradation, organic synthesis and so on for its strong oxidation and reduction abilities generated by UV light irradiation.[15–18] Hiseada group has successfully immobilized B_{12} on P25 TiO_2 or AMT600 TiO_2 nanoparticles and the obtained hybrid catalysts showed high catalytic activity for dehalogenation reactions under UV light irradiation.[19–22] In the hybrid systems, TiO_2 served not only as a catalyst support but also an effective photosensitizer. In 2011, Reisner group[23] reported a self-assembled system in which a cobalt catalyst (Et_3NH)[$Co^{III}Cl(dmgH)_2$(pyridyl-4-hydrophosphonate)] was attached on a ruthenium dye $[Ru(bpy)_3]^{2+}$-sensitized P25 TiO_2 nanoparticles. It was proved that TiO_2 played an important role as an electron mediator in the hybrid and promoted the electron transfer from the excited $[Ru(bpy)_3]^{2+}$ moieties to the cobalt catalyst under visible light irradiation. In addition, in recent years, many efforts have been focused on the photocatalytic applications of mesoporous TiO_2 microspheres for their high surface areas, suitable pore structures, and uniform pore size distributions, which could supply more active sites for adsorption and

[a]*Liaoning Key Laboratory for Green Synthesis and Preparative Chemistry of Advanced Materials, College of Chemistry, Liaoning University, Shenyang 110036, P. R. China. E-mail: weizhanghx@lnu.edu.cn; songlab@lnu.edu.cn; Fax: +86-24-62207922; Tel: +86-24-62207792*

[b]*School of Chemical Engineering, University of Adelaide, Adelaide, SA 5005, Australia*

[c]*Department of Chemistry and Biochemistry, Graduate School of Engineering, Kyushu University, Motooka, Fukuoka 819-0395, Japan*

† Electronic supplementary information (ESI) available. See DOI: 10.1039/c7ra13037f

photocatalytic reactions.[24–27] Aiming to develop more efficient photocatalyst for dechlorination, in this paper, a novel B_{12}-based hybrid catalyst co-sensitized by TiO_2 and $Ru(bpy)_3^{2+}$, B_{12}–TiO_2–Ru(II), was prepared through immobilizing a vitamin B_{12} derivative, cobyrinic acid, and a derivative of trisbipyridine ruthenium, $Ru(dcb)(bpy)_2(PF_6)_2$, on the surface of mesoporous anatase TiO_2 microspheres as shown in Fig. 1. The catalytic properties of this hybrid catalyst for 1,1-bis(4-chlorophenyl)-2,2,2-trichloroethane (DDT) dechlorination under visible light irradiation or simulated sunlight irradiation were reported. This is the first report on B_{12}-based photocatalyst co-sensitized by two photosensitizers with wide spectral response.

Experimental

Materials

1,1-Bis(4-chlorophenyl)-2,2,2-trichloroethane (DDT), $Ru(bpy)_2Cl_2$, Tetrabutyl titanate, and $Ru(bpy)_3Cl_2$ was purchased from J & K Scientific Ltd. Cyanoaqua cobyrinic acid [(CN)(H_2O)Cob(III)7COOH]Cl,[28] [(CN)(H_2O)Cob(III)7C_1ester]Cl,[19] mesoporous anatase TiO_2 microspheres,[25] 4,4′-diethyl ester-2,2′-bipyridine (deep) and $Ru(dcb)(bpy)_2(PF_6)_2$ (ref. 29) were synthesized according to the literatures. Other reagents were purchased from Sinopharm Chemical Reagent Beijing Co. (SCRC). All the reagents were of analytical grade and were used as received without further purification.

Characterization

The SEM images and EDS analysis were acquired using a Hitachi SU-8010 equipped with an EDX analyzer operated at an accelerating voltage of 5 kV. The TEM images were obtained on a JEM 2100 operating at 200 kV. The UV-vis diffuse reflectance spectroscopy (DRS) measurements were obtained on a UV-vis spectrometer (Shimadzu UV-2550) using $BaSO_4$ as a reference standard. The specific surface area of the samples was measured by the Brunauer–Emmett–Teller (BET) method using nitrogen adsorption and desorption isotherms on a Micrometrics ASAP 2020 system. The UV-vis spectra were obtained on a Perkin Elmer Lamda 25 spectrophotometer. The NMR spectra were recorded on a Mercury Vx-300 MHz NMR spectrometer. XRD patterns were obtained on a Bruker D8-Advance. The luminescence spectra were measured using a Hitachi F-4500 spectrophotometer in MeOH at room temperature. A 500 W xenon lamp (CHFXQ 500 W, Global xenon lamp power) with a $\lambda \geq 420$ nm optical filter, AM 1.5 optical filter and a heat cut-off filter provided visible light or simulated sunlight illumination.

Synthesis of $Ru(dcb)(bpy)_2(PF_6)_2$

$Ru(dcb)(bpy)_2(PF_6)_2$ was synthesized according to the literature[29] with slight modification. $Ru(bpy)_2Cl_2 \cdot 2H_2O$ (75 mg, 0.15 mmol) and 4,4′-diethyl ester-2,2′-bipyridine (44 mg, 0.15 mmol) were dissolved in ethanol (15 mL) and the mixture refluxed for 8 h. The solution was allowed to cool, filtered, and taken to dryness. The residue was dissolved in NaOH solution (0.3 mol L^{-1}, 15 mL) and refluxed for 1 h and cooled to room temperature. A large excess of NH_4PF_6 was added to the solution under vigorously stirring and then HCl (5 mol L^{-1}) was added to the mixture dropwise until much precipitate appeared. Then the precipitate was filtered and washed with a minimal amount of water, CH_2Cl_2, Et_2O respectively. After being dried in vacuum for 6 h, a dark red crystal was obtained. ^{1}H NMR (CD_3CN), δ: 7.39 (q, 4H), 7.68 (dd, 4H), 7.80 (d, 2H), 7.87 (d, 2H), 8.06 (q, 4H), 8.50 (dd, 4H), 9.19 (s, 2H).

Preparation of B_{12}–TiO_2–Ru(II)

Mesoporous anatase TiO_2 microspheres (30 mg) was added into the methanol solution (6 mL) containing [(CN)(H_2O)Cob(III)7COOH]Cl (8×10^{-4} mol L^{-1}) and $Ru(dcb)(bpy)_2(PF_6)_2$ (1.6×10^{-3} mol L^{-1}). After the mixture was stirred at room temperature for 4 h, the hybrid B_{12}–TiO_2–Ru(II) was obtained by centrifugation and washed with methanol for three times.

General catalytic procedure

A methanol solution (5 mL) containing B_{12}–TiO_2–Ru(II) (3 mg), DDT (2.4×10^{-3} mol L^{-1}) and triethanolamine (0.2 mol L^{-1}) was degassed after three of freeze–pump–thaw circles. After the solution was irradiated for 0.5 h using a xenon lamp with a $\lambda \geq 420$ nm optical filter and a heat cut-off filter or a AM 1.5 optical filter, the catalyst was separated by centrifugation. Methanol was evaporated under reduced pressure and the residue was dissolved in $CHCl_3$ (5 mL). The $CHCl_3$ layer was extracted with water (10 mL) to remove TEOA, and then the solvent was evaporated under reduced pressure to dryness. The residues were analyzed by ^{1}H NMR using 1,4-dioxane as the internal standard. The hybrid catalyst B_{12}–TiO_2–Ru(II) was washed with methanol and then reused after adding fresh triethanolamine and the substrate.

Results and discussion

Fig. 1 illustrates the preparation procedure of the hybrid B_{12}–TiO_2–Ru(II). The mesoporous anatase TiO_2 microspheres were firstly synthesized by hydrothermal reaction and then the catalyst [(CN)(H_2O)Cob(III)7COOH]Cl and the photosensitizer $Ru(dcb)(bpy)_2(PF_6)_2$ were grafted on the surface of mesoporous anatase TiO_2 microspheres through their carboxylic groups only at room temperature. After the decoration, the colour of TiO_2 microspheres changed from white to saffron yellow as shown in Fig. 1. The Co and Ru contents in the hybrid B_{12}–TiO_2–Ru(II) were 6.83×10^{-5} mol g^{-1} and 1.5×10^{-4} mol g^{-1}, which were determined through detecting the absorbance change of the characteristic peaks of [(CN)(H_2O)Cob(III)7COOH]Cl and $Ru(dcb)(bpy)_2(PF_6)_2$ at 523 nm and 480 nm respectively in the supernatant by UV-vis spectra. The Co content in this hybrid was obviously increased and was 5 times higher than that of the hybrid B_{12}–TiO_2 (AMT600) reported in the literature,[22] which should be attributed to the large surface area and pores of the mesoporous anatase TiO_2 microspheres. In addition, it is worth to mention that the ratio of Co and Ru in the hybrid was about 1 : 2.2 which was similar to their ratio 1 : 2 in the raw solution before adding TiO_2. This result indicated that the proportional co-immobilization of these two different molecules, [(CN)(H_2O)

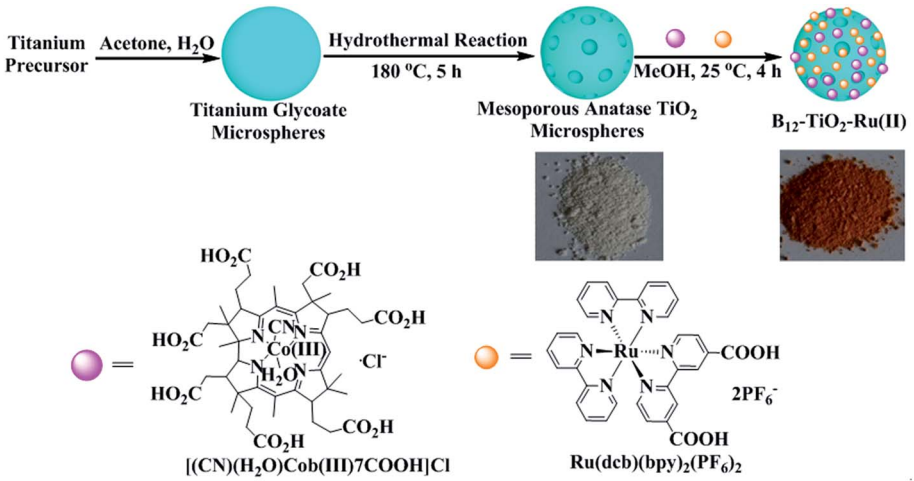

Fig. 1 Illustration of the preparation of the hybrid B_{12}–TiO_2–Ru(II).

Cob(III)7COOH]Cl and Ru(dcb)(bpy)$_2$(PF$_6$)$_2$, on the surface of TiO_2 microspheres could be easily realized by one pot reaction. In this hybrid, the Ru(II) complexes and the TiO_2 microspheres as photosensitizer are expected to be electron donors for B_{12} activation to form reactive Co(I) species.

Fig. 2 shows the UV-vis diffuse reflectance spectra of the hybrid B_{12}–TiO_2–Ru(II) and mesoporous anatase TiO_2 microsphere and the UV-vis spectra of [(CN)(H$_2$O)Cob(III)7COOH]Cl and Ru(dcb)(bpy)$_2$(PF$_6$)$_2$ in methanol. The mesoporous anatase TiO_2 microspheres strongly absorbed ultraviolet light and had very weak absorption after 400 nm.[25] The catalyst [(CN)(H$_2$O)Cob(III)7COOH]Cl exhibited a dominant absorption peak located at $\lambda_{max} = 490$ nm accompanied by a prominent shoulder located at 523 nm and a small absorption peak at 404 nm.[28] Ru(dcb)(bpy)$_2$(PF$_6$)$_2$ exhibits a broad characteristic absorptions at $\lambda_{max} = 480$ nm accompanied a small shoulder at 423 nm, which coincided with the literature.[29] Comparing with the UV-vis spectra of the above reference compounds, the broad absorption from 400 nm to 600 nm shown by the hybrid B_{12}–TiO_2–Ru(II) fully indicated that the B_{12} catalyst and the Ru(II) photosensitizer had been co-immobilized on the surface of mesoporous anatase TiO_2 microspheres successfully. The hybrid could absorb not merely ultraviolet but also visible light.

Fig. 3 gives the XRD patterns of the hybrid B_{12}–TiO_2–Ru(II) and the raw material mesoporous anatase TiO_2 microspheres. The as-prepared TiO_2 exhibited seven obviously diffraction peaks at $2\theta = 25.4°$, 37.9°, 48.1°, 55.0°, 62.8°, 68.8° and 75.0°, which corresponding to the (101), (004), (200), (211), (204), (116) and (215) crystal faces of anatase TiO_2 according to the JCPDS No. 21-1272.[25] The sharp diffraction peaks indicated that the crystallinity of the anatase TiO_2 was relatively high. After the modification with the two functional molecules, the shape and the intensity of the diffraction peaks did not change significantly, confirming that the crystallinity of the mesoporous anatase TiO_2 microspheres was well kept.

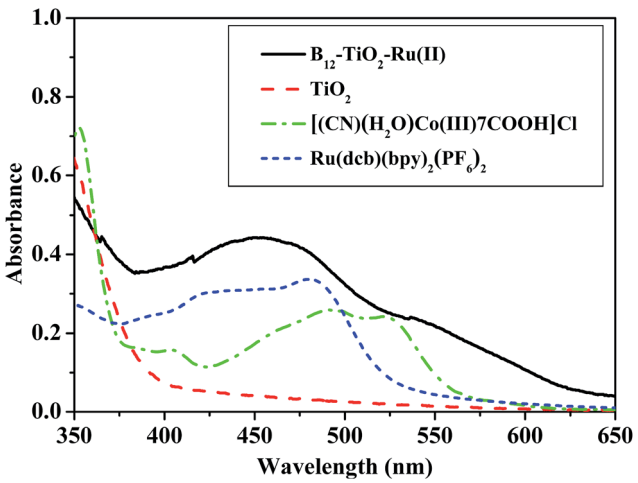

Fig. 2 UV-vis diffuse reflectance spectra of B_{12}–TiO_2–Ru(II) and TiO_2, and UV-vis spectra of [(CN)(H$_2$O)Cob(III)7COOH]Cl and Ru(dcb)(bpy)$_2$(PF$_6$)$_2$ in methanol.

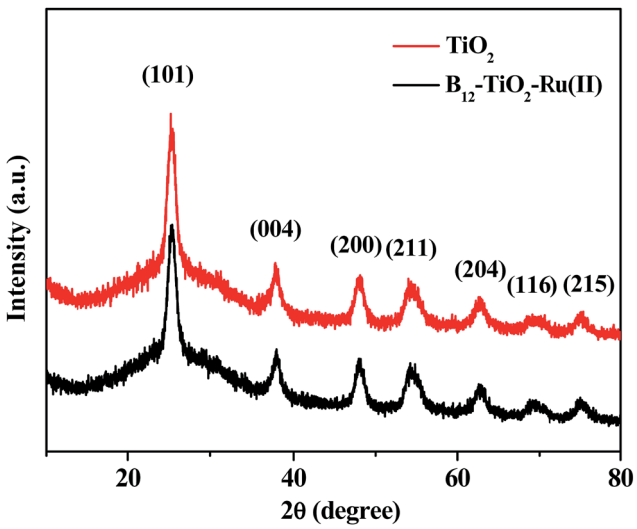

Fig. 3 XRD patterns of the hybrid B_{12}–TiO_2–Ru(II) and the raw material mesoporous anatase TiO_2 microspheres.

The morphologies and structures of the mesoporous anatase TiO_2 microspheres and the hybrid B_{12}–TiO_2–Ru(II) were characterized by SEM and TEM as shown in Fig. 4. Before or after the modification, the support TiO_2 exhibited good spherical morphology with an uniform size of about 500 nm in diameter and each TiO_2 microsphere was stacked by innumerable interconnected nanocrystals. Compared with TiO_2 nanocrystals (P25 or AMT600), the larger particle diameter could make them more easily separated from the dispersion and recycled.

The chemical composition of the hybrid B_{12}–TiO_2–Ru(II) was also determined by EDS as shown in Fig. 5. The element Ti was derived from TiO_2, while the Ru, P and F peaks arose from the photosensitizer $Ru(dcb)(bpy)_2(PF_6)_2$, Co peak originated from [(CN)(H_2O)Cob(III)7COOH]Cl and the C and N peaks originated from both $Ru(dcb)(bpy)_2(PF_6)_2$ and [(CN)(H_2O)Cob(III)7COOH]Cl. The element O was originated from $Ru(dcb)(bpy)_2(PF_6)_2$, TiO_2 and [(CN)(H_2O)Cob(III)7COOH]Cl.

High dispersity of a heterocatalyst in the reaction medium could significantly increase the effective collision probability between the catalyst and the substrate and thus promote its catalytic activity in a heterogeneous catalytic system. Therefore, the dispersity of the mesoporous TiO_2 microspheres and the hybrid B_{12}–TiO_2–Ru(II) in methanol was evaluated and the pictures were taken after standing for 1 h at room temperature. As shown in Fig. 6, both the mesoporous anatase TiO_2 microspheres and the hybrid B_{12}–TiO_2–Ru(II) dispersed well in methanol though their diameter were larger than that of the P25 or AMT600.

Nitrogen adsorption–desorption isotherms and the Barrett–Joyner–Halenda (BJH) pore-size distribution analysis are usually employed to detect structural information for porous materials. The nitrogen adsorption–desorption isotherms at 77 K of the mesoporous anatase TiO_2 microspheres and the hybrid B_{12}–TiO_2–Ru(II) are shown in Fig. 7. The as-prepared TiO_2 microspheres showed an apparent capillary condensation step at a relative pressure (P/P_0) of 0.5–0.85, which was corresponded to a pore size of 8 nm obtained by the BJH method. Their BET specific surface area was 172 $m^2\ g^{-1}$, which is three times that of P25 (ref. 19) and AMT600,[21] and the total pore volume was 0.64 $cm^3\ g^{-1}$. From the isotherms of the hybrid B_{12}–TiO_2–Ru(II), it can be confirmed that the pore size of the hybrid reduced to 7 nm and the BET specific surface area and the total pore volume decreased to 159 $m^2\ g^{-1}$ and 0.55 $cm^3\ g^{-1}$ respectively, which should be attributed to the modification of the B_{12} catalyst [(CN)(H_2O)Cob(III)7COOH]Cl and the photosensitizer $Ru(dcb)(bpy)_2(PF_6)_2$. These data indicated that the two functional molecules were immobilized not only onto the surface but also inside the pore of the TiO_2 microspheres.

Formation of the Co(I) species of the B_{12} complex in the presence of TiO_2 was monitored by the UV-vis spectral change in methanol containing a sacrificial reductant triethanolamine (TEOA) under visible light irradiation ($\lambda \geq 420$ nm). In order to avoid that the UV-vis spectral change of B_{12} in solution can't be detected sensitively after it was fixed on the TiO_2 microspheres,

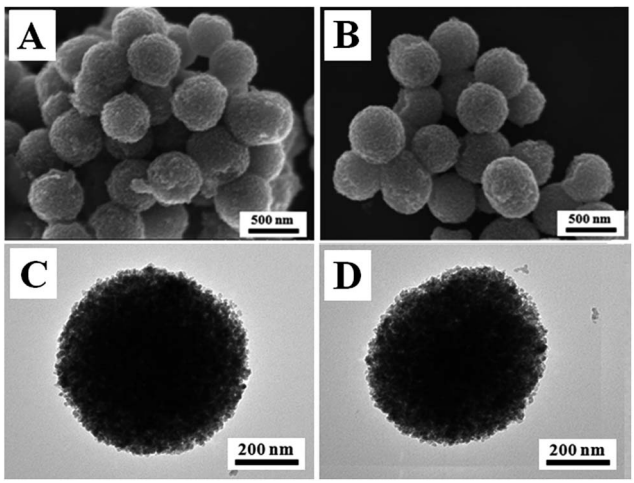

Fig. 4 SEM images of TiO_2 (A) and B_{12}–TiO_2–Ru(II) (B); TEM images of TiO_2 (C) and B_{12}–TiO_2–Ru(II) (D).

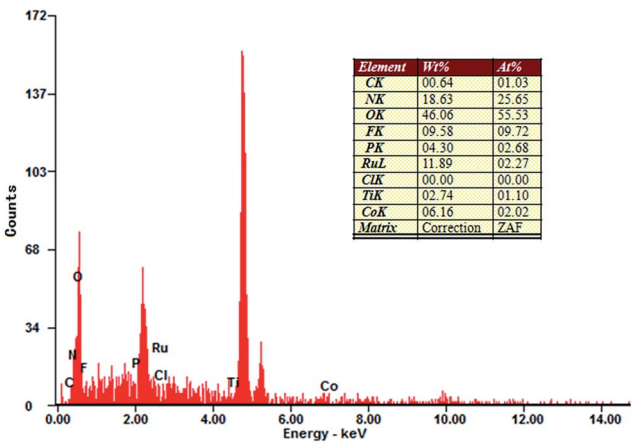

Fig. 5 EDS spectrum of the hybrid B_{12}–TiO_2–Ru(II).

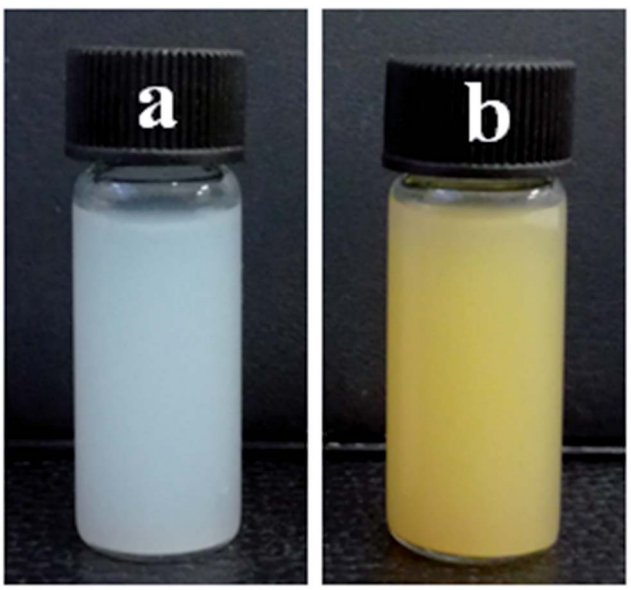

Fig. 6 Dispersions of TiO_2 (a) and B_{12}–TiO_2–Ru(II) (b) in methanol after standing for 1 h at room temperature.

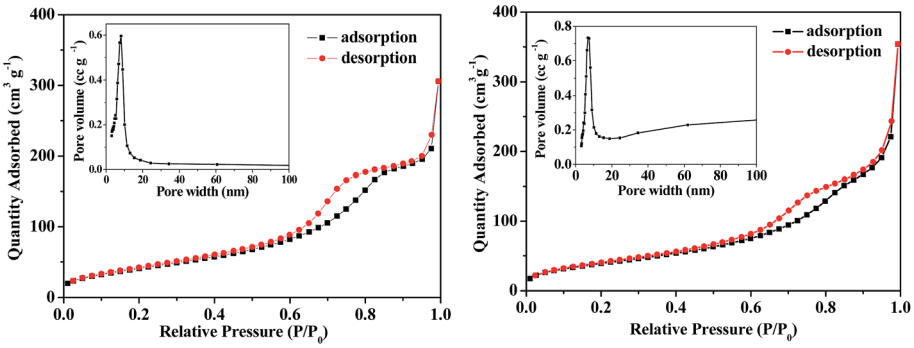

Fig. 7 Nitrogen adsorption–desorption isotherms measured at 77 K and the pore-size distribution (inset) of the mesoporous anatase TiO_2 microspheres (left) and the hybrid B_{12}–TiO_2–Ru(II) (right).

the compounds [(CN)(H_2O)Cob(III)7C_1ester]Cl and Ru(bpy)$_3$Cl$_2$ without carboxylic groups (see Fig. S1, ESI†), were used instead of [(CN)(H_2O)Cob(III)7COOH]Cl and Ru(dcb)(bpy)$_2$(PF_6)$_2$ respectively. As shown in Fig. 8a, the mixture of [(CN)(H_2O)Cob(III)7C_1ester]Cl, Ru(bpy)$_3$Cl$_2$ and TiO_2 produced three characteristic peaks at 352 nm, 463 nm and 542 nm respectively. Comparing to the UV-vis absorption spectra of [(CN)(H_2O)Cob(III)7C_1ester]Cl and Ru(bpy)$_3$Cl$_2$ (see Fig. S2, ESI†), the absorbance at 352 nm and 542 nm was assigned to the Co(III) species of the B_{12} complex and the peak at 463 nm was originated from both Co(III) and Ru(II) before irradiation. After irradiation for 25 minutes, one new peak at 392 nm was clearly observed, which was typical for the Co(I) state of the B_{12} complex,[13] and simultaneously the peaks at 352 nm and 542 nm disappeared and the absorbance at 463 nm decreased. In contrast, a slow Co(I) formation was observed in the mixture of the B_{12} catalyst and the photosensitizer without TiO_2 (Fig. 8b). Through the comparison, it was proved that the introduction of TiO_2 can efficiently promote the formation of Co(I) species, attributing to the semiconductor property of TiO_2 as an electron mediator, not only accelerating the electron transfer from the Ru(II) photosensitizer to the Co center of the catalyst, but also effectively suppressing the back electron-transfer process. When both the B_{12} catalyst and the Ru(II) photosensitizer were grafted on the TiO_2 microspheres to give a new hybrid catalyst, the distance among B_{12}, TiO_2 and Ru(II) would be sharply shortened and the electron transfer from the photosensitizer to the Co center of the B_{12} catalyst *via* TiO_2 is expected to be further accelerated under visible light irradiation.

The visible light photocatalytic activity of the hybrid B_{12}–TiO_2–Ru(II) for DDT dechlorination was investigated firstly using triethanolamine as the electron sacrificer in methanol. The results are summarized in Table 1. When using the hybrid B_{12}–TiO_2–Ru(II) as catalyst, DDT conversion was 65% only after 10 min of visible light irradiation and four kinds of dechlorinated products were obtained including one mono-dechlorinated product 1,1-bis(4-chlorophenyl)-2,2-dichloroethane (DDD, 35% yield), three di-dechlorinated products 1,1-bis(4-chlorophenyl)-2-chloroethylene (DDMU, 4% yield) and 1,1,4,4-tetrakis(4-chlorophenyl)-2,3-dichloro-2-butene (TTDB (*E*/*Z*), 9% yield), one tri-dechlorinated product methyl 2,2-bis(4-chlorophenyl) acetate (DDA methyl ester, 3% yield) (entry 1 in Table 1). When the irradiation time was increased to 30 min, not only DDT was totally converted, but also the mono-dechlorinated product DDD disappeared completely. Accordingly, the yields of the di- and tri-dechlorinated products rose and one more di-dechlorinated product 1,1-bis(4-chlorophenyl)-2-chloroethane (DDMS) was also found (entry 2 in Table 1). TTDB (*E*/*Z*) were the products of coupling reaction between two didechlorinated carbene

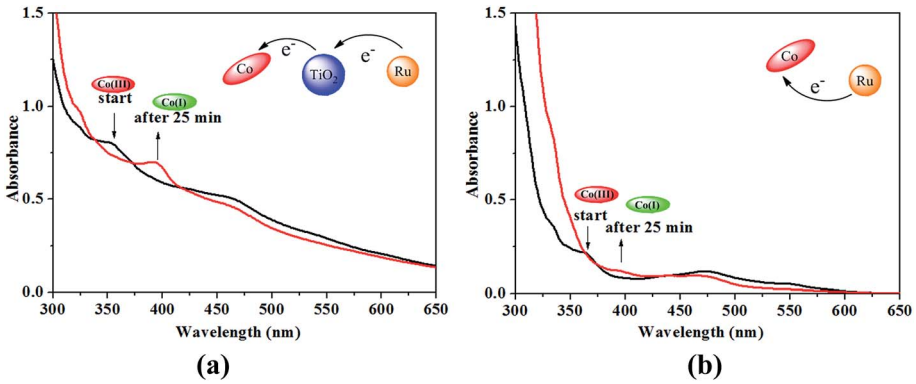

Fig. 8 UV-vis spectral change of [(CN)(H_2O)Cob(III)7C_1ester]Cl (5×10^{-6} mol L^{-1}) with TiO_2 (a) and without TiO_2 (b) in the presence of Ru(bpy)$_3$Cl$_2$ (5×10^{-6} mol L^{-1}) and TEOA (0.2 mol L^{-1}) by visible light irradiation ($\lambda \geq 420$ nm) under N_2 atmosphere in methanol.

Table 1 Photocatalytic dechlorination of DDT catalyzed by B_{12}–TiO_2–Ru(II) under visible light irradiation[a]

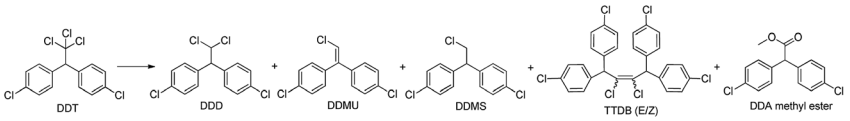

Entry	Catalytic system	Irradiation time(min)	Conversion (%)	Product yield[b] (%)					TON[c]	TOF[c] (h^{-1})
				DDD	DDMU	DDMS	TTDB (*E*/*Z*)	DDA		
1	B_{12}–TiO_2–Ru(II)	10	65	35	4	Trace	9	3	52	312
2	B_{12}–TiO_2–Ru(II)	30	100	0	40	13	20	6	119	238
3[d]	B_{12}–TiO_2–Ru(II)	30	Trace	—	—	—	—	—	0	0
4[e]	TiO_2	30	0	—	—	—	—	—	0	0
5[f]	B_{12}–TiO_2	30	24	16	—	—	—	—	9	18
6[g]	Ru(II)–TiO_2	30	13	7	—	—	—	—	—	—
7[h]	B_{12}, $Ru(bpy)_3^{2+}$	30	11	10	—	—	—	—	5	10
8[e,h]	B_{12}, $Ru(bpy)_3^{2+}$, TiO_2	30	42	21	Trace	Trace	10	Trace	30	60

[a] B_{12}–TiO_2–Ru(II) = 3 mg, [DDT] = 2.4×10^{-3} mol L^{-1}, [TEOA] = 0.2 mol L^{-1}, MeOH: 5 mL, irradiation: $\lambda \geq 420$ nm, 50 mW cm^{-2}, distance: 10 cm. [b] DDT conversion and the product yields were determined by ^1H HMR. [c] Turnover numbers (TON) and the turnover frequency (TOF) were based on the concentration of B_{12} and the product yields. [d] In the dark. [e] TiO_2 = 3 mg. [f] B_{12}–TiO_2 = 3 mg. [g] Ru(II)–TiO_2 = 3 mg. [h] $[Ru(bpy)_3Cl_2]$ = 1.1×10^{-4} mol L^{-1}, [(CN)(H_2O)Cob(III)7C_1ester]Cl = 4.9×10^{-5} mol L^{-1}.

intermediates,[12] therefore di-dechlorinated products obtained with a high yield of 93% after 30 min of irradiation, which was the highest among the B_{12}-based photocatalytic systems reported in the literatures. In addition, from the data it can be concluded that DDD could be further degraded as soon as it was produced in such a hybrid catalytic system. The reaction did not proceed under dark conditions or using TiO_2 instead of the hybrid B_{12}–TiO_2–Ru(II) (entries 3 and 4 in Table 1). When we used the hybrid B_{12}–TiO_2 or Ru(II)–TiO_2 (see Fig. S3–S5, ESI†) alone (entries 5 and 6 in Table 1), the DDT conversion decreased to 24% and 13% respectively and DDD was detected as the single product after 30 min of irradiation. In contrast to the result in the hybrid system (entry 2 in Table 1), the DDT conversion was only 11% with DDD as the single product when a 1 : 2.2 mixture of the B_{12} catalyst [(CN)(H_2O)Cob(III)7C_1ester]Cl and the photosensitizer $Ru(bpy)_3^{2+}$ was used under the same experimental conditions (entry 7 in Table 1). While adding a certain amount of mesoporous TiO_2 microspheres into the simple mixture system (entry 8 in Table 1), the DDT conversion was increased to 42% and the di-dechlorinated products TTDB (*E*/*Z*) were found with 10% yield except DDD. The results shown here indicated that after the introduction of TiO_2 to the simple mixture, especially after the co-immobilization of the B_{12} catalyst and the Ru(II) photosensitizer on TiO_2 microspheres, reaction efficiency was significantly enhanced compared to that of the simple mixture system, which should be attributed to the very important role of the mesoporous anatase TiO_2 microspheres not only as an adsorption reagent for the B_{12} catalyst, the photosensitizer and the substrate DDT or DDD *etc.* but also as an electron mediator.

TiO_2 and the Ru(II) moieties in the hybrid could be excited at the same time under sunlight irradiation because they absorb light in UV and visible region respectively. Therefore, the hybrid B_{12}–TiO_2–Ru(II) should exhibited enhanced photocatalytic activity for dechlorination under sunlight irradiation. To evaluate the co-photosensitized effect of TiO_2 and the Ru(II) complex on the B_{12} catalyst, DDT dechlorination was subsequently carried out under simulated sunlight (in Table 2). After 5 min of simulated sunlight irradiation, the DDT conversion was 49% and five dechlorinated products including DDD, DDMU, TTDB (*E*/*Z*) and DDA were found when using the hybrid B_{12}–TiO_2 alone as catalyst (entry 2 in Table 2). While using the hybrid B_{12}–

Table 2 Photocatalytic dechlorination of DDT catalyzed by B_{12}–TiO_2–Ru(II) under simulated sunlight irradiation[a]

Entry (%)	Catalyst	Irradiation time (min)	Conversion	Product yield[b] (%)					TON[c]	TOF[c] (h^{-1})
				DDD	DDMU	DDMS	TTDB (*E*/*Z*)	DDA		
1	B_{12}–TiO_2–Ru(II)	5	70	22	4	2	17	4	67	804
2	B_{12}–TiO_2	5	49	13	2	Trace	12	2	41	492
3	B_{12}–TiO_2–Ru(II)	10	100	29	15	5	19	5	173	1038
4	B_{12}–TiO_2	10	74	25	2	Trace	20	4	70	42

[a] B_{12}–TiO_2–Ru(II) = 3 mg, B_{12}–TiO_2 = 3 mg, [DDT] = 2.4×10^{-3} mol L^{-1}, [TEOA] = 0.2 mol L^{-1}, MeOH: 5 mL, irradiation illuminant: simulated sunlight, 50 mW cm^{-2}, distance: 10 cm. [b] DDT conversion and the product yields were determined by ^1H HMR. [c] Turnover numbers (TON) and the turnover frequency (TOF) were based on the concentration of B_{12} and the product yields.

Table 3 Recycled catalysis of B_{12}–TiO_2–Ru(II)[a]

Entry	Irradiation illuminant (irradiation time)	Cycle	Conversion (%)	Product yield (%)[b] DDD	DDMU	DDMS	TTDB (*E*/*Z*)	DDA
1	Visible light (30 min)	1	100	0	40	13	20	6
		2	100	0	38	14	19	7
		3	100	0	39	12	19	6
2	Simulated sunlight (5 min)	1	70	22	4	2	17	4
		2	69	23	3	1	17	3
		3	68	23	3	1	16	3

[a] B_{12}–TiO_2–Ru(II) = 3 mg, [DDT] = 2.4×10^{-3} mol L^{-1}, [TEOA] = 0.2 mol L^{-1}, MeOH: 5 mL, irradiation conditions: 50 W cm^{-2}, distance: 10 cm. [b] DDT conversion and the product yields were determined by ^{1}H HMR.

TiO_2–Ru(II) instead, the DDT conversion increased to 70% and one more product DDMS were detected (entry 1 in Table 2). When the irradiation time was prolonged to 10 min, the DDT conversion reached 100% in the hybrid B_{12}–TiO_2–Ru(II) system (entry 3 in Table 2), which was still 1.4 times that of the hybrid B_{12}–TiO_2 system (entry 4 in Table 2) and 1.5 times that of itself under visible light irradiation (entry 1 in Table 1). Comparing the data, the effect of co-photosensitization was clearly observed. TiO_2 was activated by the UV part of simulated sunlight and then transferred the electrons directly to the Co(I) center of the B_{12} catalyst, while at the same time the $Ru(bpy)_3^{2+}$ moieties in the hybrid were excited by the visible part and transferred its electrons to the Co(I) center through TiO_2. In other words, the hybrid B_{12}–TiO_2–Ru(II) realized the simultaneous utilization of both UV and visible part of the sunlight with high efficiency and the contribution of UV and visible part of the sunlight to the electron transfer has additivity.

Furthermore, the recycled catalysis of this hybrid catalyst B_{12}–TiO_2–Ru(II) under visible light irradiation and simulated sunlight irradiation was performed respectively since it can be easily separated from the reaction system by centrifugation and the relevant data were shown in Table 3. According to the data, this hybrid catalyst still kept high catalytic activity after 3 recyclings under 30 min of visible-light irradiation (entry 1 in Table 3). The recyclability of the hybrid B_{12}–TiO_2–Ru(II) at lower conversion has also been investigated under 5 min of simulated sunlight irradiation (entry 2 in Table 3). These data indicated that this hybrid catalyst had good stability and recyclability, and kept its catalytic activity after 3 recyclings even at lower conversion. The recovered B_{12}–TiO_2–Ru(II) after 3 recyclings irradiated by visible light was characterized by UV-vis spectrum and SEM respectively in Fig. 9, showing that the morphology and the optical property of the hybrid had no distinct change compared with its original.

Finally, we investigated the photosensitizing mechanism of the Ru(II) complex in the hybrid. In general, reductive and

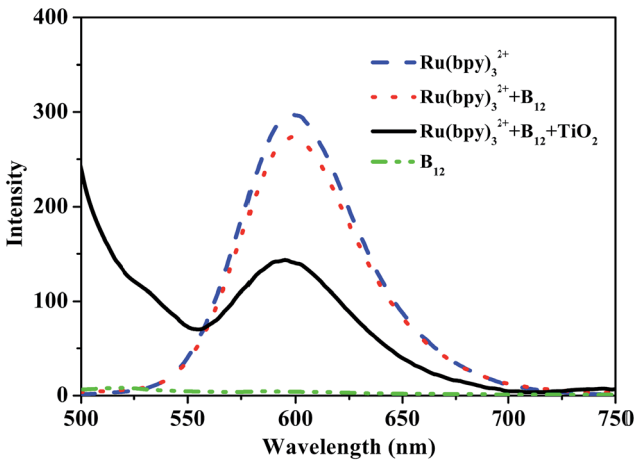

Fig. 10 The steady-state emission of $Ru(bpy)_3Cl_2$ before and after adding [(CN)(H_2O)Cob(III)7C_1ester]Cl and TiO_2 in methanol. ([$Ru(bpy)_3Cl_2$] = [[(CN)(H_2O)Cob(III)7C_1ester]Cl] = 4.7×10^{-5} mol L^{-1}, TiO_2 = 0.2 g L^{-1}, λ_{ex} = 450 nm).

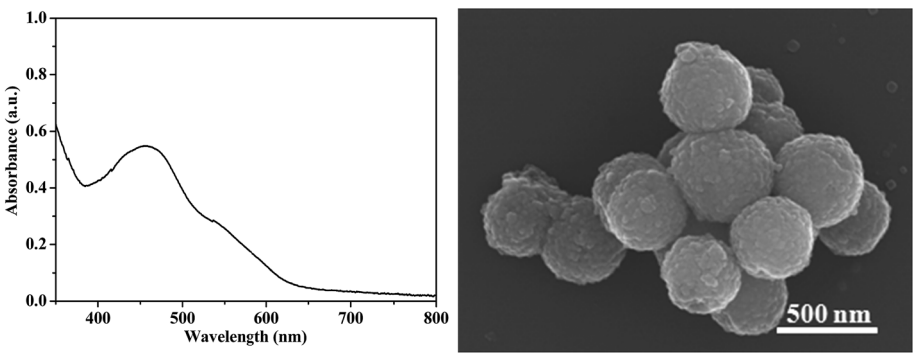

Fig. 9 UV-vis spectrum (left) and SEM (right) of B_{12}–TiO_2–Ru(II) after 3 recyclings irradiated by visible light.

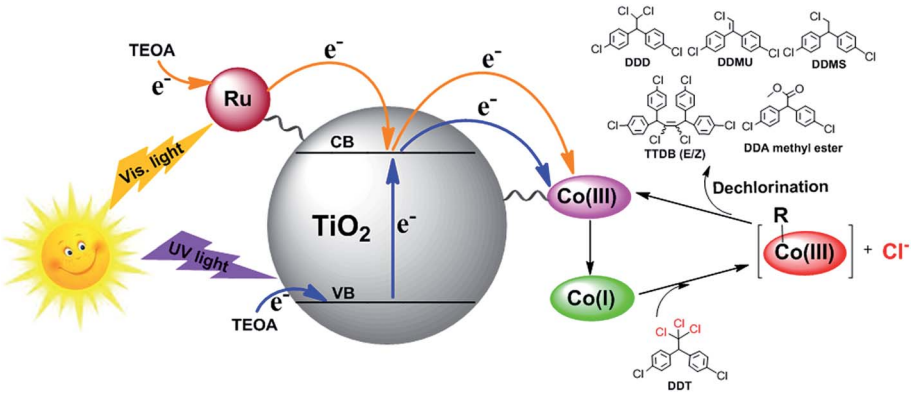

Fig. 11 Proposed mechanism for DDT dechlorination catalyzed by B_{12}–TiO_2–Ru(II) under simulated sunlight.

oxidative quenching mechanisms exist in the complex $Ru(bpy)_3^{2+}$ when it is activated by visible light irradiation.[30] To elucidate the quenching mechanism, the steady-state emission from the excited state of the Ru(II) complex before and after adding the B_{12} complex and TiO_2 was measured, as shown in Fig. 10. After exciting the metal to ligand charge transfer (MLCT) transition band of the Ru(II) complex at 450 nm, a strong emission at 600 nm was observed, while the complex [(CN)(H_2O)Cob(III)7C_1ester]Cl showed no emission at this position. After adding [(CN)(H_2O)Cob(III)7C_1ester]Cl to the solution of $Ru(bpy)_3^{2+}$, the emission intensity of the Ru(II) complexes was only slightly decreased, but if further adding a small amount of TiO_2 microspheres, the excited state of the Ru(II) complex was quenched obviously, which indicated that electron transfer should proceed efficiently between the excited state $Ru(bpy)_3^{2+}$* and TiO_2 microspheres, which is consistent with the literature.[31] Therefore, the so-called oxidative quenching mechanism could be expected for the visible-light-driven catalytic reaction in this hybrid system.

The photocatalytic mechanism of the hybrid system under sunlight was illustrated in Fig. 11. The photosensitizer $Ru(bpy)_3^{2+}$ was excited by visible light irradiation and then injected one electron to the conduction band of the support TiO_2 microspheres, and simultaneously, some electrons in the valence band of TiO_2 moved up to the conduction band under UV light irradiation. Subsequently, the Co(III) center of the B_{12} derivative accepted two electrons from the conduction band of TiO_2 and was reduced to the Co(I) species. The super-nucleophilic Co(I) species had a high reactivity with organic halides to induce the oxidative addition of the alkylating agents to the metal center with dehalogenation.[19,32] The obtained $Ru(bpy)_3^{3+}$ and the holes in the valence band of TiO_2 were rapidly reduced by the sacrificial reagent TEOA.

Conclusions

In conclusion, a B_{12}-based catalyst co-sensitized by two photosensitizers, TiO_2 and a Ru(II) complex, as a UV-vis light-driven photocatalyst was successfully synthesized. In the catalytic system composed of B_{12}–TiO_2–Ru(II) and TEOA, DDT could be completely converted into didechlorinated products and a small part was tridechlorinated only after 30 min of visible light irradiation. The catalytic activity was much higher than that of the other reported B_{12}-based photocatalytic systems. Especially, under simulated sunlight, the hybrid exhibited a significantly enhanced photocatalytic activity for dechlorination compared with B_{12}–TiO_2 at the same condition or itself under visible light irradiation attributing to the additivity in the contribution of UV and visible part of the sunlight to the electron transfer. In addition, this hybrid catalyst can be easily reused without loss of catalytic efficiency. Therefore, the presented design strategy for photocatalytic system is efficient in full utilization of solar energy and it would be readily applicable to the design of an eco-friendly catalyst.

Conflicts of interest

There are no conflicts to declare.

Acknowledgements

We are grateful for financial support from Science Foundation of Educational Department of Liaoning Province (LYB201604) and the National Natural Science Foundation of China (51773085, 21203082).

Notes and references

1 D. Friedmann, A. Hakki, H. Kim, W. Choi and D. Bahnemann, *Green Chem.*, 2016, **18**, 5391.
2 S. Klementova and M. Zlamal, *Photochem. Photobiol. Sci.*, 2013, **12**, 660.
3 M. Y. Ye, Z. H. Zhao, Z. F. Hu, L. Q. Liu, H. M. Ji, Z. R. Shen and T. Y. Ma, *Angew. Chem., Int. Ed.*, 2017, **56**, 8047.
4 X. Fan, K. Lai, L. Wang, H. Qiu, J. Yin, P. Zhao, S. Pan, J. Xu and C. Wang, *J. Mater. Chem. A*, 2015, **3**, 12179.
5 Y. Sun, W. Zhang, J. Tong, Y. Zhang, S. Wu, D. Liu, H. Shimakoshi, Y. Hisaeda and X. M. Song, *RSC Adv.*, 2017, **7**, 19197.
6 H. Tian, H. Shimakoshi, K. Imamura, Y. Shiota, K. Yoshizawa and Y. Hisaeda, *Chem. Commun.*, 2017, **53**, 9478.

7 M. Giedyk, K. Goliszewska and D. Gryko, *Chem. Soc. Rev.*, 2015, **44**, 3391.
8 K. Gruber, B. Puffer and B. Kräutler, *Chem. Soc. Rev.*, 2011, **40**, 4346.
9 H. Shimakoshi, L. Li, M. Nishi and Y. Hisaeda, *Chem. Commun.*, 2011, **47**, 10921.
10 Y. Hisaeda and H. Shimakoshi, in *Handbook of Porphyrin Science*, ed. K. M. Kadish, K. M. Smith and R. Guilard, World Scientific, 2010, vol. 10, pp. 313–370.
11 K. Tahara, H. Shimakoshi, A. Tanaka and Y. Hisaeda, *Dalton Trans.*, 2010, **39**, 3035.
12 H. Shimakoshi, M. Tokunaga, T. Baba and Y. Hisaeda, *Chem. Commun.*, 2004, **16**, 1806.
13 W. Zhang, H. Shimakoshi, N. Houfuku, X. M. Song and Y. Hisaeda, *Dalton Trans.*, 2014, **43**, 13972.
14 H. Shimakoshi, M. Nishi, A. Tanaka, K. Chikama and Y. Hisaeda, *Chem. Commun.*, 2011, **47**, 6548.
15 W. Ke, C. C. Stoumpos, J. L. Logsdon, M. R. Wasielewski, Y. Yan, G. Fang and M. G. Kanatzidis, *J. Am. Chem. Soc.*, 2016, **138**, 14998.
16 A. Romeiro, D. Freitas, M. Emilia Azenha, M. Canle and H. D. Burrows, *Photochem. Photobiol. Sci.*, 2017, **16**, 935.
17 T. Yui, A. Kan, C. Saitoh, K. Koike, T. Ibusuki and O. Ishitani, *ACS Appl. Mater. Interfaces*, 2011, **3**, 2594.
18 N. Hoffmann, *Aust. J. Chem.*, 2015, **68**, 1621.
19 H. Shimakoshi, E. Sakumori, K. Kaneko and Y. Hisaeda, *Chem. Lett.*, 2009, **38**, 468.
20 H. Shimakoshi, M. Abiru, S. Izumi and Y. Hisaeda, *Chem. Commun.*, 2009, **14**, 6427.
21 H. Shimakoshi and Y. Hisaeda, *Chempluschem*, 2014, **79**, 1250.
22 H. Shimakoshi and Y. Hisaeda, *Angew. Chem., Int. Ed.*, 2015, **54**, 15439.
23 F. Lakadamyali and E. Reisner, *Chem. Commun.*, 2011, **47**, 1695.
24 C. Guo, M. Ge, L. Liu, G. Gao, Y. Feng and Y. Wang, *Environ. Sci. Technol.*, 2010, **44**, 419.
25 Y. Zhang, S. Lin, W. Zhang, Y. Zhang, F. Qi, S. Wu, Q. Pei, T. Feng and X. M. Song, *Electrochim. Acta*, 2014, **150**, 167.
26 Y. M. Wu, M. Y. Xing, B. Z. Tian, J. L. Zhang and F. Chen, *Chem. Eng. J.*, 2010, **162**, 710.
27 Y. C. Feng, L. Li, M. Ge, C. S. Guo, J. F. Wang and L. Liu, *ACS Appl. Mater. Interfaces*, 2010, **2**, 3134.
28 K. Tahara, H. Shimakoshi, A. Tanaka and Y. Hisaeda, *Dalton Trans.*, 2010, **39**, 3035.
29 C. A. Kelly, F. Farzad, D. W. Thompson, J. M. Stipkala and G. J. Meyer, *Langmuir*, 1999, **15**, 7047.
30 A. Juris, V. Balzani, F. Barigelletti, S. Campagna, P. Belser and A. V. Zelewsky, *Coord. Chem. Rev.*, 1988, **19**, 85.
31 E. E. Beauvilliers and G. J. Meyer, *Inorg. Chem.*, 2016, **55**, 7517.
32 H. Shimakoshi, Y. Nagami and Y. Hisaeda, *Appl. Chem. Eng.*, 2015, **4**, 9.